Mössbauer Effect in Metallic Iron*

R. S. PRESTON, S. S. HANNA, AND J. HEBERLE
Argonne National Laboratory, Argonne, Illinois

(Received July 26, 1962)

The Mössbauer effect in metallic iron has been studied from 4 to 1300°K, with particular emphasis on the region near the Curie temperature at 1043°K.

Measurements of the internal field H_n at the nucleus agree with nuclear magnetic resonance measurements and follow closely, but not exactly, the saturation magnetization curve of iron. No internal field is observed above the Curie temperature. At room temperature $H_n=330\pm3$ kOe. The ratio of magnetic moments of the two lowest levels of Fe^{57} is $\mu_1/\mu_0=-1.715\pm0.004$.

The observed temperature shift in the energy of the resonant radiation may be attributed chiefly to relativistic time dilation. In the low-temperature region the variation is nonlinear and compatible with a Debye temperature $\theta=400\pm30$°K, although the data indicate that θ is not strictly independent of temperature. At high temperatures, the classical limit $(1/E)\partial E/\partial T=-3k/2Mc^2$ for the relativistic shift is attained and perhaps exceeded. Disagreement with the classical limit would indicate a temperature variation in the isomer shift. At the Curie point and at the transition from α to γ iron, the discontinuities observed in the temperature shift are too great to be attributed to the relativistic shift. If attributed to the isomer shift, these discontinuities indicate that the electron density at the nucleus increases at the transitions from the ferromagnetic to the paramagnetic state and from α to γ iron.

The strength of the resonant absorption was also determined as a function of temperature. These measurements are compatible with a Debye temperature that falls from about 400 to 300°K in passing from low to high temperatures over the range studied.

I. INTRODUCTION

THE discovery of the recoilless emission and absorption of nuclear gamma radiation by Mössbauer[1] in 1958 has provided a powerful means of investigating many phenomena in nuclear and solid-state physics which previously could not be studied at all, or at best only with difficulty and low precision. This method has had its most striking successes in the case of the first excited state of Fe^{57} at 14.4 keV.[2–4] The importance of the Mössbauer effect in Fe^{57} is due not only to the fact that its great strength and sensitivity make it the most favorable case discovered so far, but also to the propitious circumstance that iron and many of its compounds and alloys are ferromagnetic. Thus, one is provided with a sensitive tool for the study of ferromagnetism.

The property most vividly revealed by the Mössbauer effect in a ferromagnetic material is the existence of the large magnetic field at the nucleus,[5–7] a cooperative effect of the polarized atomic electrons. The observation, measurement, and interpretation of the magnetic splittings of the two lowest nuclear levels of Fe^{57} have been reported in a series of papers.[8–11] In pure iron the internal field at the nucleus has a value of about 330 kOe at room temperature,[10] its direction is opposite to the direction of magnetization,[11] and its temperature dependence is very similar to that of the spontaneous magnetization.[12,13] Because of the directional correlation between the internal field and the magnetization, the Mössbauer radiation can easily be polarized[9] by magnetizing the iron and thereby aligning the domains and the internal fields.

It is the intention of this work to present a more detailed account of the Mössbauer effect in metallic Fe^{57}, with special emphasis on the variation with temperature. Three quantities have been measured as a function of temperature: (1) the internal field at the nucleus, (2) the shift in energy between source and absorber, and (3) the strength of the resonant absorption. In each case these measurements can be related to the temperature dependence of other significant properties of the solid state. Particular attention has been paid to the behavior of these quantities at and near the Curie temperature of iron, where the magnetization vanishes.

The spectrum of the radiation emitted (or absorbed) by the 14.4-keV level of Fe^{57} in metallic form presents

* Work performed under the auspices of the U. S. Atomic Energy Commission.

[1] R. L. Mössbauer, Z. Physik **151**, 124 (1958).

[2] J. P. Schiffer and W. Marshall, Phys. Rev. Letters **3**, 556 (1959).

[3] R. V. Pound and G. A. Rebka, Jr., Phys. Rev. Letters **3**, 554 (1959).

[4] G. de Pasquali, H. Frauenfelder, S. Margulies, and R. N. Peacock, Phys. Rev. Letters **4**, 71 (1960).

[5] W. Marshall, Phys. Rev. **110**, 1280 (1958); R. E. Watson and A. J. Freeman, ibid. **123**, 2027 (1961).

[6] A. C. Gossard and A. M. Portis, Phys. Rev. Letters **3**, 164 (1959).

[7] M. A. Grace, C. E. Johnson, N. Kurti, R. G. Scurlock, and R. T. Taylor, Communications, *Conference de Physique des Basses Temperatures Paris, 1955* (Centre National de la Recherche Scientifique and UNESCO, Paris, 1956), p. 263; N. E. Alekseevsky, N. V. Zavaritsky, and I. F. Shchegolev, quoted by G. R. Khutsishvili, Zhur. Eksptl. i Teoret. Fiz. **29**, 894 (1955).

[8] S. S. Hanna, J. Heberle, C. Littlejohn, G. J. Perlow, R. S. Preston, and D. H. Vincent, Phys. Rev. Letters **4**, 28 (1960).

[9] G. J. Perlow, S. S. Hanna, M. Hamermesh, C. Littlejohn, D. H. Vincent, R. S. Preston, and J. Heberle, Phys. Rev. Letters **4**, 74 (1960).

[10] S. S. Hanna, J. Heberle, C. Littlejohn, G. J. Perlow, R. S. Preston, and D. H. Vincent, Phys. Rev. Letters **4**, 177 (1960).

[11] S. S. Hanna, J. Heberle, G. J. Perlow, R. S. Preston, and D. H. Vincent, Phys. Rev. Letters **4**, 513 (1960).

[12] S. S. Hanna, J. Heberle, R. S. Preston, and D. H. Vincent, reported in "Mössbauer Effect, Allerton House Conference Proceedings," TN60-698, 1960, p. 39.

[13] D. E. Nagle, H. Frauenfelder, R. D. Taylor, D. R. F. Cochran, and B. T. Matthias, Phys. Rev. Letters **5**, 364 (1960).

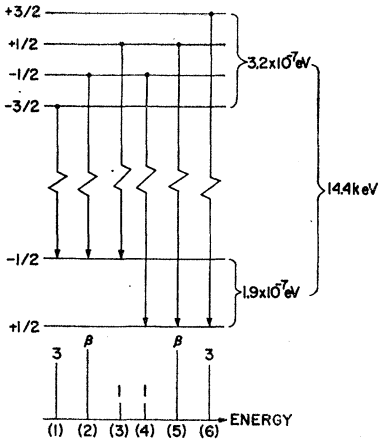

FIG. 1. Zeeman splittings of the two low levels of Fe^{57} by the internal magnetic field at the nucleus in ferromagnetic iron. The transitions are those appropriate to magnetic-dipole radiation.

a simple example of a pure nuclear Zeeman effect. Because of the cubic symmetry of the iron lattice, there can be no quadrupole shifts in the nuclear energy levels. Moreover, as it turned out, the radiation is almost entirely magnetic-dipole in character[10,14] so that there are only six lines in the Zeeman pattern, as shown in Fig. 1. The relative intensities of the transitions are[15]

$$I_1=I_6=3(1+\cos^2\theta),$$
$$I_2=I_5=4\sin^2\theta,$$
$$I_3=I_4=1+\cos^2\theta,$$

where θ is the angle between the magnetic field and the direction of propagation of the radiation. Lines 3 and 6 in Fig. 1 have right elliptical polarizations with ellipticities equal to $\cos\theta$; lines 1 and 4 have left elliptical polarizations with ellipticities equal to $\cos\theta$; and lines 2 and 5 are linearly polarized perpendicular to the direction of the field.

At $\theta=90°$ the intensity pattern is 3:4:1:1:4:3, with linear polarizations $\|, \perp, \|, \|, \perp, \|$. For $\theta=0$ the pattern changes to 3:0:1:1:0:3, with circular polarizations left, right, left, right for the four lines of nonzero intensity. If the magnetic domains (and, hence, the internal fields) are randomly oriented, then the radiation is unpolarized and the intensities are 3:2:1:1:2:3, as follows from averaging the above intensities over all angles. If the sample is partially magnetized, then, for propagation at right angles to the average direction of magnetization, the ratio is $3:\beta:1:1:\beta:3$, where β is between 2 and 4 and depends on the degree of magnetization.

In the early work done with iron,[10] both the source and the absorber were metallic iron, so that the nuclear levels were split in both environments and a rather complicated resonant absorption spectrum was produced. Subsequently, it has been customary to use a source (or absorber) that is not ferromagnetic, so that a single line is emitted (or absorbed) and the six-line spectrum of Fig. 1 is displayed directly in the resonant absorption spectrum.[16] The splittings in this spectrum are simply related to $\mu_0 H_n$ and $\mu_1 H_n$, where H_n is the magnetic field at the nucleus and μ_0 and μ_1 are the magnetic moments of the ground state and first excited state, respectively.

In Marshall's treatment[5] of the origin of the internal field H_n in the 3d transition group, it is implicit that H_n is proportional to the atomic magnetic moment and hence to the saturation magnetization σ, i.e., that

$$H_n=a\sigma. \tag{1a}$$

However, H_n is not produced directly by the polarized d electrons but rather by the s electrons which, though only slightly polarized by the d electrons, have large densities at the nucleus. Thus

$$H_n=a'[|\psi\downarrow(0)|^2-|\psi\uparrow(0)|^2], \tag{1b}$$

where $|\psi\downarrow(0)|^2$ and $|\psi\uparrow(0)|^2$ denote the densities (at the nucleus) of s electrons with spin down and up, respectively, relative to the magnetization. The experimental result that the coefficient a in Eq. (1a) is negative corresponds to having $|\psi\downarrow(0)|^2<|\psi\uparrow(0)|^2$ in Eq. (1b).

The location of the center of gravity of the resonant-absorption spectrum measures the difference in energy between the emission process and the absorption process. This energy difference arises from two causes: the so-called temperature shift[17,18] and the isomer (or chemical) shift.[19]

The temperature shift arises because of the time dilations resulting from the motions of the emitting and absorbing nuclei.[17] The shift in energy of radiation emitted by the source is

$$\Delta E/E=-\tfrac{1}{2}(\langle v_s^2\rangle_{\rm av}/c^2), \tag{2a}$$

where $\langle v_s^2\rangle_{\rm av}$ is the mean-square velocity of nuclei in the source. Relative to the absorber, the shift is

$$\Delta E/E=(1/2c^2)[\langle v_a^2\rangle_{\rm av}-\langle v_s^2\rangle_{\rm av}], \tag{2b}$$

where a denotes the absorber. Since the mean-square velocities are functions of temperature, it is often convenient to use a temperature coefficient defined by

$$(1/E)(\partial E/\partial T)=-(1/2c^2)(\partial/\partial T)\langle v^2\rangle_{\rm av}. \tag{3a}$$

If harmonic lattice forces are assumed, this expression becomes

$$(1/E)(\partial E/\partial T)=-C_L/2Mc^2, \tag{3b}$$

where M is the atomic mass and C_L the specific heat of the lattice. In the high-temperature limit, the coefficient

[14] G. T. Ewan, R. L. Graham, and J. S. Geiger, Nuclear Phys. 19, 221 (1960).
[15] See, for example, L. W. Fagg and S. S. Hanna, Revs. Modern Phys. 31, 711 (1959).
[16] S. L. Ruby, L. M. Epstein, and K. H. Sun, Rev. Sci. Instr. 31, 580 (1960).
[17] R. V. Pound and G. A. Rebka, Jr., Phys. Rev. Letters 4, 274 (1960).
[18] B. D. Josephson, Phys. Rev. Letters 4, 341 (1960).
[19] O. C. Kistner and A. W. Sunyar, Phys. Rev. Letters 4, 412 (1960).

becomes rigorously

$$(1/E)(\partial E/\partial T)=-3k/2Mc^2. \tag{3c}$$

The isomer shift arises because the Coulomb interaction between an atomic electron and the nucleus depends on the size of the nucleus. For a uniform distribution of charge within a nuclear radius R the shift of a nuclear energy level[20,21] is $\frac{2}{5}\pi Ze^2R^2|\psi(0)|^2$, where $|\psi(0)|^2$ is the total s-electron density at the nucleus. If the radii of the ground state and excited state are different, then the gamma-ray energy is changed by an amount

$$\Delta E=\tfrac{2}{5}\pi Ze^2|\psi(0)|^2(R_1^2-R_0^2). \tag{4}$$

This shift will be different in source and absorber if $|\psi(0)|^2$ is different and will vary with temperature if $|\psi(0)|^2$ is sensitive to temperature.

Finally, the strength of the resonant absorption can be obtained from the area A above the dips in the transmission curve normalized to unity far off resonance. For an isolated absorption line having a Lorentzian shape of width Γ, this area is either[22]

$$A=\tfrac{1}{2}\pi n f_s f_a \sigma_0 \Gamma G(n f_a \sigma_0) \tag{5a}$$

or

$$A^2=\pi n f_s^2 f_a \sigma_0 \Gamma^2 F(n f_a \sigma_0), \tag{5b}$$

independent of the shape of the emission line and instrumental broadening. The first expression is appropriate for thin absorbers, the second for thick ones. The functions G and F, given in graphical form by Havens and Rainwater,[22] have the properties $G(0)=1$ and $F(\infty)=1$. The thickness of the absorber is denoted by n expressed in nuclei per cm^2. The cross section σ_0 is the on-resonance value of the absorption cross section for gamma radiation. Thus

$$\sigma=\sigma_0/\{[(2/\Gamma)(E-E_0)]^2+1\}, \tag{6a}$$

$$\sigma_0=2\pi\lambda^2\omega/(1+\alpha), \tag{6b}$$

where ω is a statistical factor [equal to $(2J_1+1)/(2J_0+1)$ for upper and lower states with spins J_1 and J_0], α is the internal-conversion coefficient, and the other quantities have their conventional meanings.

The presence of f_a in Eqs. (5a) and (5b) takes account of the fact that some nuclei do not take part in the recoilless absorption, so that the number of nuclei in the absorber is effectively $f_a n$. In similar fashion f_s appears in these expressions since the measured area A must be renormalized to A/f_s to account for the nuclei that do not take part in recoilless emission in the source. The Mössbauer fraction f_a or f_s is given by[23]

$$f=\exp[-\tfrac{1}{3}(E_0^2/c^2)\langle r^2\rangle_{\rm av}]=e^{-2W}, \tag{7a}$$

where $\langle r^2\rangle_{\rm av}$ is the mean-square displacement of the nuclei. For a Debye solid, W becomes the Debye-Waller factor

$$W=3(E_R/k\theta)[\tfrac{1}{4}+(T/\theta)^2\phi(T/\theta)]. \tag{7b}$$

In this expression $E_R=E_0^2/2Mc^2$ is the energy of free recoil of the nucleus of mass M, θ is the Debye temperature, and ϕ is a tabulated integral.[24]

In the present investigation, an isolated line is found only above the Curie point. Below the Curie point there are six lines whose overlap depends on the temperature so that the analysis of the areas must be modified accordingly.

II. EXPERIMENTAL PROCEDURE

A. Source

A monochromatic source was obtained by plating approximately 1 mC of Co^{57} onto a pure copper foil,[25] and then diffusing the radioactive material into the metal by heating it in hydrogen at 800°C for 1 h and then in vacuum ($\approx 4\times10^{-6}$ mm Hg) at 800°C for 2 h. Such a source has been used by the Harwell group[26] and is known to emit radiation in a single line. In the work reported here, the source was mounted in vacuum on the bottom of a container filled with liquid nitrogen. By means of this arrangement the source was maintained at a constant and readily reproducible temperature, as was essential for the measurements. The radiation emerged from the cryostat through a Mylar window 1 mil thick. When this source was used with a natural iron absorber at a temperature above the Curie point ($fn\sigma<1$), the width of the observed line was 1.5 times the expected natural width.

B. Absorber

For most of the work the absorber was a foil of metallic iron enriched[27] to 53.6% in Fe^{57}. These foils were cut from a sheet rolled to a nominal thickness of 0.1 mil, a typical thickness being 1.66 mg/cm^2. For the early runs no special effort was made to purify the iron after preparation from the material supplied by Oak Ridge. However, it became evident that the resonant-absorption spectrum just below the Curie temperature consisted of a single line superimposed on a six-line spectrum (Fig. 5). This suggested the presence of a nonmagnetic phase of iron and therefore of an appreci-

[20] I. Solomon, Compt. rend. **250**, 328 (1960).
[21] L. R. Walker, G. K. Wertheim, and V. Jaccarino, Phys. Rev. Letters **6**, 98 (1961).
[22] W. W. Havens, Jr., and L. J. Rainwater, Phys. Rev. **83**, 1123 (1951); E. Melkonian, W. W. Havens, Jr., and L. J. Rainwater, *ibid.* **92**, 702 (1953); S. S. Hanna and L. Meyer-Schützmeister, *ibid.* **115**, 986 (1959).
[23] W. Marshall and J. P. Schiffer (unpublished note); K. S. Singwi and A. Sjölander, Phys. Rev. **120**, 1093 (1960).
[24] M. W. Holm, Atomic Energy Commission Research and Development Report IDO-16399, 1957 (unpublished); A. H. Compton and S. K. Allison, *X-rays in Theory and Experiment* (D. Van Nostrand Company, Inc., Princeton, New Jersey, 1935), p. 437.
[25] The plated source was supplied by Nuclear Science and Engineering Corporation, Pittsburgh, Pennsylvania.
[26] C. E. Johnson, M. S. Ridout, T. E. Cranshaw, and P. E. Madsen, Phys. Rev. Letters **6**, 450 (1961).
[27] The enriched iron was supplied by the Isotopes Division of Oak Ridge National Laboratory.

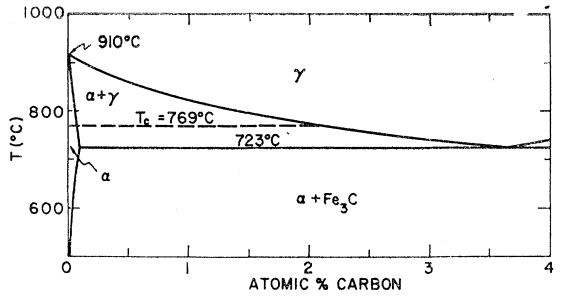

FIG. 2. Phase diagram for the iron-carbon system, in the high-temperature region and for small carbon content. Adapted from data in M. Hansen, *Constitution of Binary Alloys* (McGraw-Hill Book Company, Inc., New York, 1958), pp. 353–359.

able impurity which was assumed to be carbon. Calculations from the phase diagram of iron (Fig. 2) show, for example, that a 0.5% carbon impurity would cause 10% of the iron to go abruptly into the nonmagnetic γ phase on reaching a temperature of 720°C, and that the fraction in the γ phase would then increase to 20% as the temperature rose to the Curie point (770°C).

Subsequently, carbon was removed from the absorber foils by heating at 900°C in a stream of electrolytic hydrogen which had been bubbled through water to moisten it.[28] After three hours at about 900°, the foil was cooled rapidly to prevent a slight blueing which otherwise would have occurred as it passed through 300°C, probably because of residual impurities in the hydrogen.

Chemical analyses on thick (0.013 in.) natural iron foils showed that an initial 0.1% carbon contamination was reduced to 0.002% by this procedure. One of these purified test foils was placed in the vacuum furnace (Sec. II E) in such a way that it did not interfere with the passage of gamma rays through the absorber. The foil remained in the furnace during ten days of running at temperatures ranging between 700° and 1000°. A later analysis of this test foil showed that it contained 0.004% carbon, which represents an insignificant increase.

The Mössbauer measurements themselves give additional evidence for the continued high purity of the iron during experimentation. Figure 6 shows that the nonmagnetic phase is certainly greatly reduced just below the Curie point in the purified iron. Also, Fig. 9 shows that at about 910°C the temperature shift has a discontinuity, which indicates an abrupt phase change. The change from α to γ phase is known to occur at this temperature in pure iron. Referring again to the Fe-C phase diagram, Fig. 2, it is seen that a carbon impurity of as little as 0.1% would produce a *gradual* change from the α to the γ phase, starting at about 720° and ending a few degrees below 910°, with no sudden jump at 910°.

[28] R. M. Bozorth, *Ferromagnetism* (D. Van Nostrand Company, Inc., Princeton, New Jersey, 1951), pp. 60–66.

C. Detector

The 14.4-keV radiation was detected with a NaI crystal, 2 in. in diam and 40 mils thick. After amplification, the 14.4-keV pulses were selected with a single-channel analyzer and registered in a scaler. A 256-channel analyzer was used, from time to time, to monitor the gain and stability of the system.

D. Velocity Drive

The device used to move the source in order to obtain the velocity spectra was the carriage and lead screw of a lathe, as in our previous work.[8–11] This mechanical method was selected, because it provides a simple and absolute measurement of velocity, with stability over short and long periods of time. Also the source can easily be held at a constant and reproducible temperature, since it can be housed in a cryostat (Sec. II A) that is separate from the fixed absorber.

The cryostat containing the source was mounted on the lathe carriage which moved back and forth at a constant preset speed. The effective distance of travel was defined by a microswitch at each end of the stroke. These switches actuated two scalers receiving the 14-keV pulses from the detector. One scaler was used to record pulses when the source was moving toward the absorber, and the other was used when the motion was reversed. In identical fashion the same microswitches actuated two other scalers receiving pulses from a 100-kc/sec crystal oscillator (stepped down to 5 kc/sec). In this manner, the total transmitted intensity of 14-keV radiation and the total time were recorded, for a positive and a negative velocity of equal magnitudes, during a run which typically consisted of many round trips of the source. The effective distance was determined by making static measurements on the positions at which the microswitches operated. It is believed that the absolute velocity measurements are accurate to about 0.2%. The motor of the lathe was reversed at each end by means of a second microswitch placed an adequate distance beyond the microswitch that operated the scalers. At one end, a third microswitch recorded the number of round trips.

For a few special measurements it was convenient to replace the mechanical drive by an electronic vibrator and to accumulate the velocity spectrum as a whole instead of point by point.[29]

E. Vacuum Furnace

A specially constructed vacuum furnace was employed (Fig. 3) to produce high temperatures in the absorber. The body of the furnace is a hollow stainless steel cylinder. The absorber is clamped near the center between two disks of beryllium oxide (each 0.4 mm

[29] This instrument was constructed by F. J. Lynch and J. B. Baumgardner and is described in Argonne National Laboratory Report ANL-6391, 1961 (unpublished), p. 10.

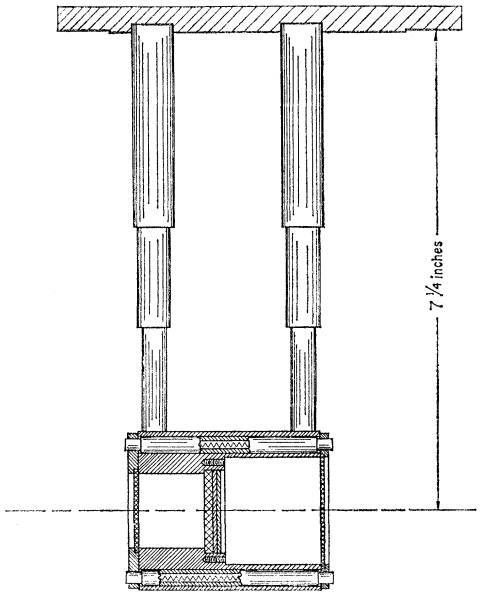

FIG. 3. Furnace used to heat the absorber in vacuum. The various materials are given in the text.

thick). An adjacent disk of boron nitride (1.4 mm thick) holds two thermocouple junctions. The ends of the cylindrical cavity are covered with thin (0.8 mm) disks of boron nitride so as to form an isothermal enclosure. The furnace is heated by eight coiled tungsten heaters (made of wire 0.35 mm in diam) inserted into alumina tubes embedded in the cylindrical wall of the furnace.

The furnace is suspended from a brass cover plate by means of two stainless steel tubes. The bottom section of each tube has a wall thickness of only 0.008 in. to reduce heat loss by conduction. The plate holding the furnace is the lid of a water-cooled vacuum can provided with two Mylar windows (each 1 mil thick) for transmission of the 14-keV gamma rays. The Mylar windows are shielded from the thermal radiation of the furnace by thin (0.25 mm) sheets of beryllium. The maximum temperature attained in the furnace was 1300°K at a heater power of about 1 kW.

F. Cryostats

For measurements from room temperature to liquid-nitrogen temperature, the absorber was mounted in a cryostat similar to that holding the source (Sec. II A). For the measurements at liquid-helium temperature, the absorber was mounted on the bottom of a liquid-helium vessel. The thermal-radiation shield, cooled by liquid nitrogen, contained two 0.005-in. aluminum foil windows to transmit the gamma rays.

G. Measurement of Temperature

Below room temperature, the temperature of the absorber was measured to an accuracy of ±1°C by use of a copper-constantan thermocouple screwed to the frame holding the absorber.

At room temperature and above, the two thermocouples used had junctions of platinum and platinum-rhodium (10%) alloy. The hot junction of each couple was clamped between the boron-nitride disk and the beryllium oxide disk on one side of the absorber foil. One hot junction was at the center, the other at the edge of the disks. The external cold junctions were kept in ice water. The calibrations of the thermocouples were not exactly the same and, occasionally, they changed—as was evident from the readings at the Curie point T_c. These changes were attributed to absorption of impurities, probably from the boron nitride disk. When from time to time the old junctions were cut off and new junctions were formed, the original thermocouple readings at T_c were nearly restored. It was usually possible to hold the temperature to within ±0.2°C during a day's run.

In effect, the Curie point was used to calibrate the thermocouples at appropriate times during the investigation. It is especially important to have a precise knowledge of temperatures near T_c, where the internal field at the nucleus varies rapidly with temperature. In this temperature region, therefore, the thermocouples were calibrated at the beginning of each day. In practice T_c was determined quickly by setting the source velocity at the known location of the center of the single resonance for temperatures just above T_c. Then the absorber temperature was allowed to fall slowly through the range of thermocouple readings known to contain T_c. The transmission was measured at intervals of a fraction of a degree, and was plotted as a function of thermocouple reading as shown in Fig. 7. The rise in the curve is attributed to the appearance of the magnetic splitting at T_c. As pointed out in Sec. III A, the temperature is not strictly constant across the absorber foil, so that the break in the curve is not ideally sharp.

H. Analysis of Data

The complete absorption spectrum was measured, usually twice, at each setting of the absorber temperature. Observations were made at velocity intervals of approximately 0.2 mm/sec, or less. A typical run at low temperature required 36 speed settings (producing 72 positive and negative velocities). Approximately 60 000 counts were obtained for each velocity.

For each run below the Curie temperature, the data were fitted with a spectrum of either six Lorentzian or six Gaussian lines by means of a least-squares analysis, performed with the aid of a program[30] developed for an IBM-704 computer. Although instrumental broadening of the experimental lines was not negligible, better fits were obtained with the Lorentzian than with the Gaussian shape. Therefore, the final values of the

[30] A description of this program is available and may be obtained from J. P. Schiffer, Argonne National Laboratory.

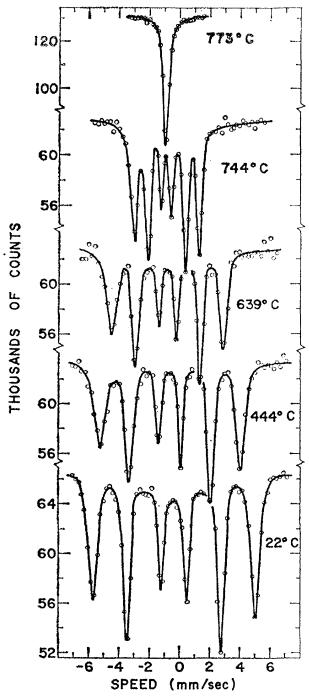

FIG. 4. Typical spectra for metallic Fe^{57} between room temperature and the Curie temperature. The single-line source (Co^{57} in Cu) was at the temperature of liquid nitrogen.

parameters were obtained with the former. The parameters obtained for each line were the width, the depth, and the velocity at the center. To allow for the possibility of a velocity-dependent base line, the counting rate off resonance was fitted with the function $y=y_0(1+k_1v+k_2v^2)$, where v is the velocity.

At temperatures above the Curie point the fit was, naturally, to a single line rather than six. For runs below room temperature the absorber was clamped between beryllium metal disks which had a sufficient iron impurity to produce an additional weak resonance. Data from these runs, therefore, were fitted with a seven-line spectrum.

The computer program permits the application of various constraints during the calculation. For instance, the value of any parameter may be fixed, or any linear relationship among the parameters may be specified. Thus, the computer can be required to make the best fit with the proviso that the separations between lines 1 and 2, 2 and 3, 4 and 5, and 5 and 6 be equal. This constraint corresponds to the situation expected for cubic symmetry of the absorber lattice. This expectation was confirmed at low temperatures where the imposition of this constraint gave a separation which was not significantly different from the average separation of the lines as calculated without such a constraint. In order to obtain the splittings and their errors directly, it was decided to apply this constraint in the analysis of all the data. At temperatures just below the Curie point, where the lines are poorly resolved, it was especially convenient to use this constraint to speed up the machine calculation. At these temperatures it was also worth while to specify that the ratio of the splittings of the ground state and first excited state be the same as the average value computed from the low-temperature runs.

The results of the machine calculation for each experimental run include values of all the parameters, an error matrix for the parameters, and the value of χ^2 for the fit. Through the use of χ^2 and the error matrix, realistic values of the probable error can be obtained for each parameter separately, or for any function of one or more of the parameters. Typically, χ^2 was two to three times the expected value. This probably reflects the fact that the experimental lines were not strictly Lorentzian.

The reliability of the standard deviations derived from the machine calculations may be judged by comparing the calculated standard deviation σ of some quantity measured in a single run with the actual rms deviation from the mean of values of this quantity as measured in many runs. A useful quantity for such a comparison is the ratio of the magnetic moments of the first excited state and ground state in Fe^{57}. This ratio is $\mu_1/\mu_0=-3\bar{g}_1/\bar{g}_0$, where $\bar{g}_1$ is the splitting in the excited state and $\bar{g}_0$ the splitting in the ground state. The average value of μ_1/μ_0 determined from 34 runs at temperatures between 4 and 913°K is -1.715. The rms deviation from -1.715 is 0.004. The error matrices for the individual runs give values of σ ranging between 0.003 and 0.0055 with an average of $\sigma=0.004$ which agrees with the rms value.

III. RESULTS

A. Spectra

Figure 4 shows typical spectra for temperatures, from room temperature to the Curie point T_c. The collapse of

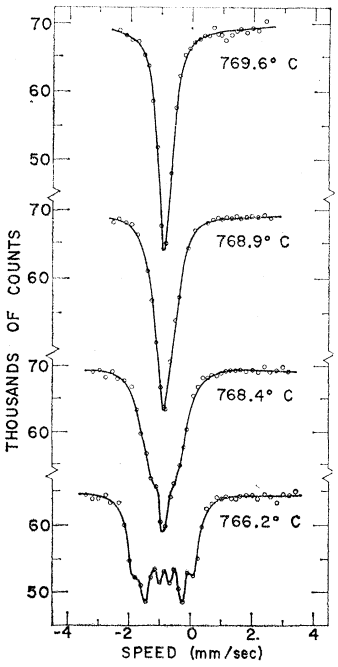

FIG. 5. Spectra in the region of the Curie temperature for an unpurified foil of metallic Fe^{57}. The central component visible just below T_c =773°C indicates some nonmagnetic γ phase of iron, present because of a carbon impurity.

TABLE I. Numerical results for a foil of unpurified iron (53.6% Fe^{57})0.2×10^{-3} cm thick. The splittings of the ground state and excited state are designated by g_0 and g_1, respectively. The listed values can be converted to Mc/sec by multiplying by 11.57. The average errors in g_0 and g_1 are ±0.008 and ±0.005 mm/sec, respectively. The internal field at the nucleus is given under H_n. These values were computed with $E_\gamma=14.37\pm0.01$ keV and $\mu_0=0.0903\pm0.0007$ nm. The error in H_n is about ±3 kOe. The center of gravity of the spectrum, S_T, is referred to its value S_0 at absolute zero. Values can be converted to $\Delta E/E$ by dividing by c (in mm/sec). The average error in S_T is ±0.003 mm/sec. The Curie point was found at a thermocouple reading corresponding to about 1045°K. The absolute error in T ranges from about 1° to 3° in going from low to high temperature.

T (°K)	g_0 (mm/sec)	g_1 (mm/sec)	H_n (kOe)	(S_T-S_0) (mm/sec)
293.9	3.922	2.245	330	−0.116
372.6	3.870	2.216	326	−0.169
497.4	3.758	2.137	315	−0.249
613.7	3.585	2.053	302	−0.330
718.0	3.385	1.942	285	−0.402
816.0	3.111	1.782	262	−0.479
912.5	2.684	1.539	226	−0.547
1019.0	1.558	0.903	133	−0.626
1040.3	—	—	70.0	−0.638
1043.7	—	—	36.9	−0.655
1046.0	0	0	0	−0.650
1048.1	...	...	...	−0.656

the internal field is vividly portrayed in this sequence. Figure 5 shows spectra in the vicinity of T_c for an unpurified foil. Figure 6 is a similar sequence of spectra for a foil purified in the manner described in Sec. II b. It is apparent that just below T_c the nonmagnetic γ phase is much less prevalent after purification of the foil. The small central component still visible below T_c in the purified foil results primarily from a temperature gradient in the absorber foil (i.e., a portion of the foil probably is actually above T_c). At temperatures from T_c to 1275°K only a single line without structure was observed. The disappearance of structure at T_c was also studied by means of observations such as those shown in Fig. 7.

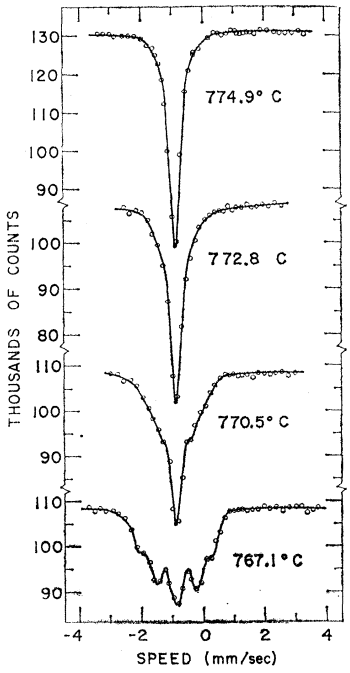

FIG. 6. Spectra in the region of the Curie temperature for a purified foil of metallic Fe^{57}. The nonmagnetic component is removed or at least greatly reduced. The central component here is due primarily to the fact that part of the foil is actually above the Curie temperature.

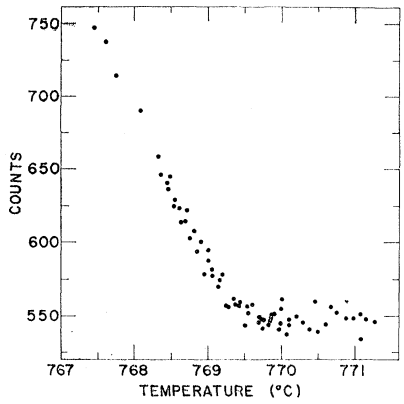

FIG. 7. Temperature dependence of the transmission, measured at a velocity corresponding to maximum absorption just above T_c. The rather abrupt change in transmission occurs at T_c and results from the complete vanishing of magnetic splitting above T_c.

Numerical results obtained from the analysis of the data are listed in Tables I–III.

B. Magnetic Moment of the Excited State

As noted above, the value found for μ_1/μ_0 is -1.715 ± 0.004. With $\mu_0=\pm0.0903\pm0.0007$ nm, as obtained by Ludwig and Woodbury,[31] one obtains $\mu_1=-0.1549\pm0.0013$ nm.

TABLE II. Numerical results for a foil of purified iron (53.6% Fe^{57}) 1.66 mg/cm² thick. See Table I for description of headings and average errors. The Curie point was found at about 1042°K.

T (°K)	g_0 (mm/sec)	g_1 (mm/sec)	H_n (kOe)	(S_T-S_0) (mm/sec)
293.0	3.924	2.244	330	−0.117
717.6	3.377	1.927	284	−0.402
912.3	2.687	1.537	226	−0.546
1019.2	1.559	0.891	131	−0.628
1039.4	0.732	0.427	62.4	−0.640
1041.6	—	—	29.0	...
1042.1	0	0	0	−0.641
1042.8	...	...	...	−0.648
1043.4	...	...	...	−0.637
1046.1	...	...	...	−0.652
1054.6	...	...	...	−0.666
1084.6	...	...	...	−0.683
1104.7	...	...	...	−0.697
1124.3	...	...	...	−0.712
1144.7	...	...	...	−0.728
1164.8	...	...	...	−0.741
1184.9	...	...	...	−0.754
1205.0	...	...	...	−0.798

[31] G. W. Ludwig and H. H. Woodbury, Phys. Rev. **117**, 1286 (1960).

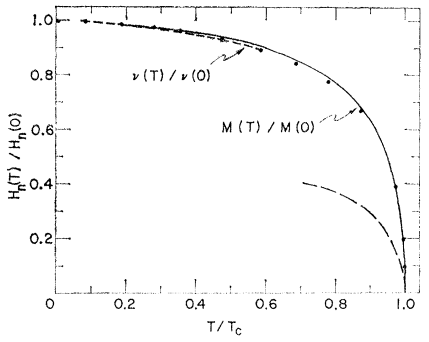

FIG. 8. Internal magnetic field $H_n(T)$, normalized to the value $H_n(0)$ at absolute zero, plotted as a function of the ratio of the foil temperature to the Curie temperature T_c. The dots represent the Mössbauer measurements. The solid line is the saturation magnetization measured by Potter. The upper dashed line summarizes the NMR measurements. The lower dashed line shows the temperature dependence on a temperature scale expanded tenfold.

C. Internal Magnetic Field

The internal magnetic field at the nucleus $H_n(T)$ is proportional to the total splitting in the spectrum, i.e., to the difference in the positions of lines 6 and 1 in Fig. 1. Values of $H_n(T)/H_n(0)$ obtained from these splittings are plotted as a function of T/T_c in Fig. 8. Also plotted in Fig. 8 is the curve obtained by Potter[32] for the spontaneous magnetization of iron, and the curve obtained by nuclear magnetic resonance (NMR) by Robert and Winter[33] and by Koi *et al.*[34] for the frequency corresponding to the ground-state splitting of Fe^{57}. In order to obtain a fair comparison, all the data are normalized to the same value (0.97) at room temperature.

The internal field, as measured by the Mössbauer effect, appears to fall off more rapidly with increasing temperature than does the magnetization, as measured by Potter. The discrepancy is outside the limit of error of the Mössbauer measurements, but may be within the uncertainty of the magnetization measurements. On the other hand, the Mössbauer measurements of the internal field agree very well with the NMR measurements. The agreement is actually better than can be depicted in Fig. 8. Because of the narrower line width, the NMR measurements are somewhat more precise than the Mössbauer measurements.

The lower dashed curve in Fig. 8 shows the variation of the internal field with the abscissae expanded tenfold. This curve emphasizes the sudden vanishing of the field at T_c, which is evident in Fig. 7 as well as from the fact that no structure or broadening has been observed in any spectrum obtained above T_c.

TABLE III. Numerical results at low temperatures for the foil that was used to obtain the data in Table II. The experimental arrangement differed slightly in the two experiments. See Table I for description of headings and average errors.

T (°K)	g_0 (mm/sec)	g_1 (mm/sec)	H_n (kOe)	(S_T-S_0) (mm/sec)
≈4	4.015	2.290	338	0
82	4.002	2.286	337	−0.005
198	3.964	2.271	334	−0.057
298	3.912	2.232	329	−0.118
370	3.860	2.202	324	−0.162

[32] H. H. Potter, Proc. Roy. Soc. (London) **A146**, 362 (1934).
[33] C. Robert and J. M. Winter, Compt. rend. **250**, 3831 (1960).
[34] Y. Koi, A. Tsujimura, T. Hihara, and T. Kushida, J. Phys. Soc. Japan **16**, 1040 (1961).

D. Temperature Shift

The location of the center of gravity of the absorption spectrum is plotted as a function of the temperature in Fig. 9. The rather sharp breaks in the curve at T_c and at the temperature of the α-γ phase transition should be noted.

The discontinuity at T_c was unexpected, but has been confirmed by a series of measurements in the vicinity of T_c. The absorber was maintained at a temperature such that part of the foil was actually below and part above T_c (see Sec. III A), the spread in temperature being only a few degrees. Under these conditions, the spectrum exhibits a sharp component superimposed on a broad component, as shown in Fig. 10. In order to minimize possible distortion of the spectral shape, these data were obtained with the source mounted on the electronic vibrator,[29] and the spectrum was accumulated as a whole, instead of point by point. The least-squares analysis of the data in Fig. 10 shows that, relative to the broad component, the sharp component is shifted by 0.11±0.06 mm/sec. This shift, which was observed in many runs similar to that of Fig. 10, confirms the discontinuity shown in Fig. 9.

If the possibility of a temperature-dependent isomer shift is ignored, then according to Eq. (3b) the slope of the curve in Fig. 9 at a given temperature is proportional to the lattice specific heat at that temperature. From a value of zero at 0°K, the slope in Fig. 9 increases

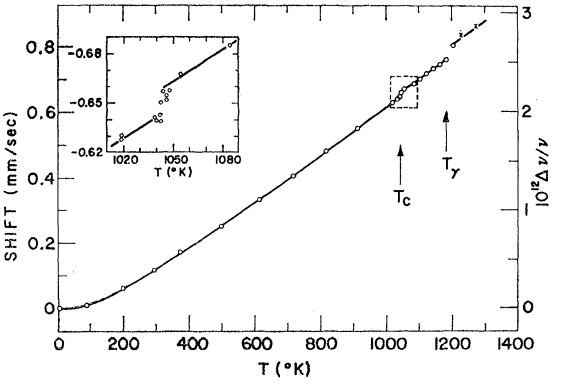

FIG. 9. Temperature shift in the spectrum of metallic Fe^{57}. The shift is arbitrarily set equal to zero at absolute zero. The Curie temperature and the temperature of the α-γ phase transition are designated by T_c and T_γ, respectively. The insert shows a magnified view of the measurements in the vicinity of T_c.

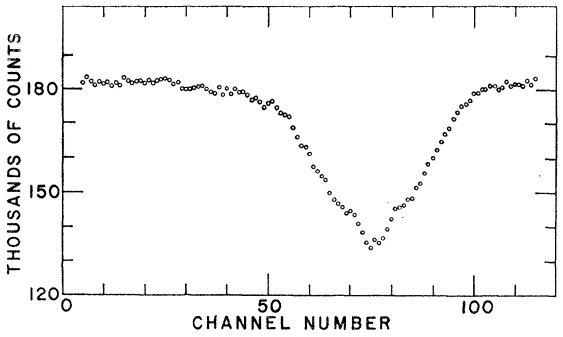

FIG. 10. Spectrum of metallic Fe^{57} with part of the absorber foil above and part below the Curie temperature. The sharp component ($T>T_c$), is shifted to the right relative to the broad component ($T<T_c$). Note that the velocity scale is reversed in this figure.

with increasing temperature in qualitative agreement with the variation in the specific heat of a Debye solid. At high temperatures the curve becomes linear with a slope agreeing closely with the classical value corresponding to $C_L=3k$ [Eq. (3c)]. Values of the slope at room temperature, and below and above the Curie temperature, are given in Table IV.

The slope at room temperature agrees well with the value of $(2.09\pm0.05)\times10^{-15}$ obtained by Pound *et al.*[35] These authors have also measured the pressure coefficient of the shift and have used it to compute the slope at constant volume. In accordance with their procedure, measurements on the temperature shift were converted from constant pressure to constant volume by means of the relation

$$\frac{1}{\nu}\left(\frac{\partial\nu}{\partial T}\right)_V=\frac{1}{\nu}\left(\frac{\partial\nu}{\partial T}\right)_P-\frac{1}{\nu}\left(\frac{\partial\nu}{\partial \ln V}\right)_T\left(\frac{\partial \ln V}{\partial T}\right)_P.$$

At room temperature, the conversion term is

$$\frac{1}{\nu}\left(\frac{\partial\nu}{\partial \ln V}\right)_T\left(\frac{\partial \ln V}{\partial T}\right)_P=(4.48\times10^{-12})(35.3\times10^{-6}\text{ per °K})$$
$$=0.16\times10^{-15}\text{ per °K}.$$

The value for $(1/\nu)(\partial\nu/\partial \ln V)_T$ was derived from values of $(1/\nu)(\partial\nu/\partial P)_T$ and $(\partial P/\partial \ln V)_T$ measured by Pound *et al.*[35] and Bridgman,[36] respectively. The value of

TABLE IV. Temperature coefficients of resonant radiation from metallic Fe^{57}. The values listed are in units of 10^{-15} per °K.

T (°K)	$\frac{1}{\nu}\left(\frac{\partial\nu}{\partial T}\right)_P$	$\frac{1}{\nu}\left(\frac{\partial\nu}{\partial T}\right)_V$
295	-2.09 ± 0.06	-2.25 ± 0.07
718–1019	-2.45 ± 0.06	-2.63 ± 0.07
1054–1185	-2.32 ± 0.06	-2.50 ± 0.07

[35] R. V. Pound, G. B. Benedek, and R. Drever, Phys. Rev. Letters **7**, 405 (1961).
[36] P. W. Bridgman, Revs. Modern Phys. **18**, 1 (1946).

TABLE V. Mössbauer cross sections and Debye temperatures for metallic iron.

Method	T (°K)	$f\sigma_0$ (10^{-18} cm^2)	θ_D (°K)
Temperature shift	293	···	400 ± 30
Absorption vs thickness	293	2.3 ± 0.4	···
Absorption vs thickness	1050	0.60 ± 0.06	310 ± 15
Absorption vs temperature	0–700	···	≈400
Absorption vs temperature	1050–1200	···	≈300

$(\partial \ln V/\partial T)_P$ was obtained from Basinski *et al.*[37] Thus, at room temperature the temperature coefficient at constant volume becomes

$$(1/\nu)(\partial\nu/\partial T)_V=-(2.25\pm0.07)\times10^{-15}\text{ per °K},$$

corresponding to a Debye temperature of 400°K. This Debye temperature is in rather good agreement with values measured by other means[24] and is perhaps not greatly different from the value derived from the strength of the resonant absorption (Table V).

In the high-temperature region ($T\approx1000$°K),

$$\frac{1}{\nu}\left(\frac{\partial\nu}{\partial \ln V}\right)_T\left(\frac{\partial \ln V}{\partial T}\right)_P=(4.33\times10^{-12})(41.0\times10^{-6}\text{ per °K})$$
$$=0.18\times10^{-15}\text{ per °K}.$$

The value of 4.33×10^{-12} was obtained by writing

$$\frac{1}{\nu}\left(\frac{\partial\nu}{\partial \ln V}\right)_T=\frac{1}{\nu}\left(\frac{\partial\nu_{\text{isom}}}{\partial \ln V}\right)_T+\frac{1}{\nu}\left(\frac{\partial\nu_{\text{rel}}}{\partial \ln V}\right)_T$$

and assuming the isomeric term to have its room-temperature value[35] of 4.27×10^{-12} and the relativistic term to be reduced to 0.06×10^{-12} (in accordance with the Debye model) from its room-temperature value of 0.21×10^{-12}. The relativistic term, which was calculated for $\theta=400$°K, is small enough that the value of the conversion term (0.18×10^{-15} per °K) would be practically unchanged over a wide range of choices for θ.

With this conversion term the temperature coefficient at constant volume becomes $(-2.63\pm0.07)\times10^{-15}$ per °K and $(-2.50\pm0.07)\times10^{-15}$ per °K, just below and just above the Curie point, respectively, as listed in Table IV.

E. Energy of Gamma Ray

The conversion from a velocity spectrum to an energy spectrum is effected through the relation

$$\Delta v/c=\Delta E/E.$$

At 20°C the average value of Δv for the splitting of the ground state is 3.921 ± 0.005 mm/sec. The splitting ΔE of the ground state, according to the NMR measure-

[37] Z. S. Basinski, W. Hume-Rothery, and A. L. Sutton, Proc. Roy. Soc. (London) **A229**, 459 (1955).

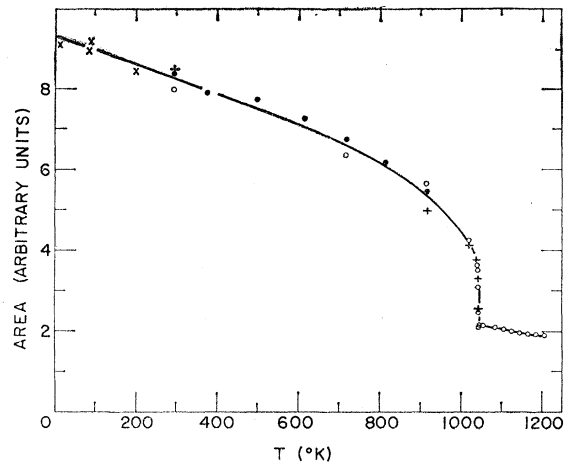

FIG. 11. Total area above the absorption dips, plotted as a function of the temperature for a metallic Fe^{57} absorber. The data are a composite of several runs and are only qualitative, but they indicate the striking effect of the vanishing of the splitting in the spectrum.

ment of Koi *et al.*,[34] is 45.49±0.03 Mc/sec, corresponding to $(1.883\pm0.001)\times10^{-7}$ eV. When these values are substituted, the Doppler-shift formula yields $E_\gamma=14.40\pm0.03$ keV. This may be compared with the value 14.37±0.01 keV obtained by Bellicard and Moussa,[38] who measured the energy of the conversion electrons ejected in the decay of the level. In other words, the NMR value for the internal magnetic field is the same as that obtained with the Mössbauer measurements, to within the uncertainties of the measurements.

It is necessary, however, to be cautious in making absolute comparisons of the internal fields, since we have found that this field may vary by as much as 0.5% in different specimens. The slight systematic change in the values of the field in Table III as compared with the values in Tables I and II may be evidence of this variation. There is evidence, however, that a unique value of the field is obtained if the specimen is purified and annealed as described in Sec. II B.

F. Mössbauer Fraction

The total area above the transmission dips, as obtained from the least-squares analyses, is plotted in Fig. 11 as a function of temperature. The coalescence of 6 lines into a single line produces a marked change in the area, as is graphically portrayed by these data. The thickness of the absorber for the single line above the Curie point is six times the average thickness for the six lines below the Curie point. Since the absorption increases roughly as the square root of the thickness, the total area is considerably reduced.

The solid curve in Fig. 11 is a visual fit. However, it was compared with theoretical curves computed for exponential absorption by six overlapping Lorentzian lines whose spacings at any given temperature were set equal to the observed spacings. An internal-conversion coefficient of 10 was assumed in these calculations (see below). Up to about 700°K the shape of the curve is compatible with a Debye temperature of about 400°K. Above about 700°K the Debye temperature apparently falls, reaching a value around 300°K in the region above the Curie temperature.

Since the data in Fig. 11 are a composite of several runs made without careful control of the relevant parameters, more accurate determinations of the Mössbauer fractions were carried out at room temperature and just above the Curie point by measuring the areas for a thin, a medium, and a very thick absorber. The measurements were analyzed by the ratio method. If subscripts 1 and 2 refer to two different absorbers, then from Eq. (5b) the ratio of the areas is

$$\left(\frac{A_2}{A_1}\right)^2=\frac{n_2F(n_2f_a\sigma_0)}{n_1F(n_1f_a\sigma_0)}. \tag{8}$$

Since A_2, A_1, n_2, and n_1 are measured and F is a known function, this relation determined $f_a\sigma_0$. In practice n_1 and n_2 are determined by weighing the absorbing foils and measuring their areas. The areas A_1 and A_2 above the transmission dips are obtained from the measured transmission curves normalized to unity far off resonance. This normalization requires a knowledge of the nonresonant background radiation recorded by the detector. Fortunately, only the ratio of the areas is required, and the ratio is rather insensitive to the background correction. In obtaining the area above a transmission dip, it is not sufficient to use the area of the best-fitting Lorentzian curve, since the dips become increasingly non-Lorentzian for thick absorbers and the method depends on the comparison of a thin and a thick absorber. To obviate this difficulty, least-squares Lorentzian fits were made to transmission dips theoretically computed for each absorber thickness used. The ratio of the Lorentzian area to the true area was computed and this factor was then used to correct the Lorentzian areas obtained from the empirical curves. Figure 12 illustrates the ratio method for a set of measurements made just above the Curie point. The corrected ratios A_2/A_1 are plotted against n_2/n_1. A reasonable fit to the data is obtained for $n_1f_a\sigma_0=1.0\pm0.1$, which gives $f_a\sigma_0=(0.60\pm0.06)\times10^{-18}$ cm². Simi-

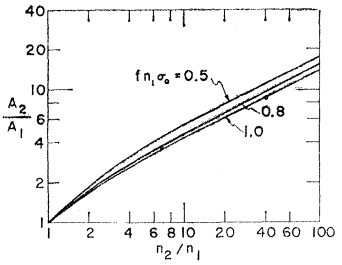

FIG. 12. Ratio of areas plotted against ratio of absorber thicknesses for $T=778$°C. The curves are theoretical curves obtained from Eq. (8).

[38] J. B. Bellicard and A. Moussa, J. phys. radium **18**, 115 (1957)

lar measurements and analyses at room temperature yield $f_a\sigma_0=(2.3\pm0.4)\times10^{-18}$ cm². These measurements confirm the trend of the data in Fig. 11.

The resonant cross section σ_0 may be calculated from Eq. (6b) if λ, ω, and α are known. Unfortunately, two values of α have been reported,[39,40] 15±1 and 9.94±0.60, so that f_a and hence the Debye temperature θ, as defined by Eqs. (7a) and (7b), cannot be obtained with any precision from the above measurements. This is especially true at low temperatures ($T<300$°K) where θ is very sensitive to f so that it will require very refined measurements to obtain meaningful values of θ.

However, the measurement at room temperature can be used to obtain an upper limit for α. Thus if $f_a\leqslant1$, $\sigma_0\geqslant1.9\times10^{-18}$ cm² which gives $\alpha\leqslant12$. This result indicates that $\alpha=9.94\pm0.60$ is probably the better measurement. If this value is accepted, then at $T\approx T_c$, $\theta=310\pm15$, which is the value listed in Table V.

IV. DISCUSSION

A. Magnetic Moments

The observed magnetic moments of the two lowest levels of Fe^{57} are both anomalously small. The shell-model values for $p_{1/2}$ and $p_{3/2}$ neutron orbits are 0.64 and −1.91 nm, respectively, as compared with the measured values of 0.09 and −0.15 nm in Fe^{57}. Since the latter values are an order of magnitude smaller, it would appear that the agreement in sign is largely fortuitous and that there is a great deal of configuration mixing in Fe^{57}. Lawson and MacFarlane[41] have considered a rotational model for Fe^{57}. They found that it is not difficult to select a nuclear deformation that will give the excited-state moment as well as other significant properties of Fe^{57}, but that the ground-state moment cannot be obtained in any reasonable way. Hamamoto and Arima[42] have studied a shell-model description of Fe^{57} involving neutron orbits $2p_{3/2}$, $2p_{1/2}$, and $1f_{5/2}$ and have achieved some success in fitting the magnetic moments of the two levels. It must be remarked that any successful model of Fe^{57} must also fit a rather large body of other experimental data in addition to the magnetic moments.

B. Internal Magnetic Field

Benedek and Armstrong[43] have made a careful study of the explicit constant-volume temperature dependence of the quantity A in the relation

$$\nu=A\sigma,$$

where ν is the NMR frequency of Fe^{57}. Below 600°K they find

$$A=A_0(1-0.77\times10^{-7}T^2). \tag{9}$$

As noted in Secs. III C and III E above, while the internal field H_n is not exactly proportional to the saturation magnetization σ, the NMR and Mössbauer measurements of H_n are in very good agreement with each other (Fig. 8). Therefore it must be assumed that a in Eq. (1a) also has an explicit temperature dependence of the form (9). Hence, according to Eq. (1b), the polarizability of s electrons $(1/\sigma)[|\psi_\downarrow(0)|^2-|\psi_\uparrow(0)|^2]$ depends explicitly on temperature. The agreement between the NMR and Mössbauer measurements is noteworthy because the NMR measurements are associated with nuclei within the domain walls[44] while the Mössbauer measurements involve chiefly nuclei within the domains themselves.

The disappearance of an effective internal field above the Curie temperature, as noted in Sec. III C, indicates the absence of any short-range cooperative phenomena above T_c, but it is clear that only a short-range order that persists longer than 10^{-7} sec, the nuclear lifetime, would be observed in these measurements.

C. Temperature Shift

As $T\rightarrow\infty$ the relativistic part of the temperature coefficient must approach $3k/2Mc^2=2.44\times10^{-15}$ per °K [Eq. (3c)]. The experimental value just below T_c appears to be above this classical limit. If this is so, the discrepancy may be attributed to an explicit temperature dependence of the isomer shift, i.e., $(1/\nu)(\partial\nu_{\text{isom}}/\partial T)_V\approx-0.2\times10^{-15}$, in contrast to the room-temperature value[35] which is $<0.1\times10^{-15}$.

The transition from α to γ iron occurs in a region in which the relativistic temperature shift has substantially attained its classical value given by Eq. (2b) with $\langle v_a^2\rangle_{\text{av}}=3kT/M$. Therefore, the discontinuity (≈0.03 mm/sec) observed at the α-γ transition is much too large to be attributed to a jump which the relativistic shift might make as a result of a difference of Debye temperatures in the two phases. Hence, it is necessary to invoke a discontinuity in the isomer shift, i.e., in the electron density at the nucleus. The magnitude of the discontinuity is comparable to shifts that have been observed for Fe^{57} nuclei diffused into neighboring d-group metals.[21] The sense of the shift indicates [Eq. (4)] that the density of s electrons at the nucleus increases in going from the α to the γ phase of iron.

Similarly it is not possible to account for the discontinuity (≈0.01 mm/sec) at the Curie temperature by any reasonable jump in the relativistic shift. If instead

[39] H. R. Lemmer, O. J. A. Segaert, and M. A. Grace, Proc. Phys. Soc. (London) **A68**, 701 (1955).
[40] H. C. Thomas, C. F. Griffin, W. E. Phillips, and E. C. Davis, Jr., Bull. Am. Phys. Soc. **7**, 120 (1962).
[41] R. D. Lawson and M. H. MacFarlane, Nuclear Phys. **24**, 18 (1961). See also J. F. Vervier and G. A. Bartholomew, *Proceedings of the International Conference on Nuclear Structure, Kingston, September 1960* (North-Holland Publishing Company, Amsterdam, 1960), p. 650.
[42] I. Hamamoto and A. Arima, Nuclear Phys. **37**, 457 (1962).
[43] G. B. Benedek and J. Armstrong, Suppl. J. Appl. Phys. 32, 106S (1961).
[44] A. M. Portis and A. C. Gossard, Suppl. J. Appl. Phys. **31**, 205S (1960).

it is attributed to the isomer shift, the sense indicates again an increase in electron density in going above the Curie temperature.

D. Debye Temperature

The measurements indicate that the Debye temperature is not constant in iron. It should be noted that at low temperatures the best value of θ probably comes from measurements of the temperature shift, while at high temperatures it is necessary to rely on absorption measurements. However, the shift measurements involve $\langle v^2\rangle_{\text{av}}$ [Eq. (2a)] while the absorption measurements involve $\langle r^2\rangle_{\text{av}}$ [Eq. (7a)]. The degree of agreement to be expected between the effective Debye temperatures calculated from these two quantities depends on the extent to which iron approximates a Debye solid. On the other hand, both methods appear to agree in the low-temperature region (Table V). More refined measurements will be needed to test this agreement further.

ACKNOWLEDGMENTS

It is a pleasure to acknowledge the assistance of T. R. Hart in accumulating and analyzing the data. D. H. Vincent and Elsa Meints-Garmire participated in some of the preliminary measurements. We have profited from discussions with our colleague, John Schiffer, who was also instrumental in obtaining the program for analysis of the data. We are grateful to F. J. Karasek for preforming the iron foils and to F. J. Lynch and J. B. Baumgardner for the construction of the electronic vibrator used in some of the work. Our understanding of many points and our enthusiasm have been greatly strengthened by extended discussions with Walter Marshall.

PHYSICAL REVIEW VOLUME 128, NUMBER 5 DECEMBER 1, 1962

Comparison of the Rubidium-87 and Proton Zeeman Transition Frequencies in the Earth's Magnetic Field

P. L. BENDER*
National Bureau of Standards, Washington, D. C.
(Received June 21, 1962)

Alternate measurements of the earth's magnetic field have been made at the same location with a dc rubidium-87 magnetometer and with a proton free-precession magnetometer. The accuracy of the measurements is believed to be 1 μG in terms of the rubidium-87 frequency and 3 μG in terms of the proton frequency. The ratio of the g factors for rubidium electrons and for protons in a spherical water sample is found to be 658.234±0.004. The rubidium electron g factor is thus 27±6 parts per million higher than the g factor for electrons in the hydrogen ground state.

I. INTRODUCTION

A COMPARISON of the rubidium electronic g factor and the proton g factor has been obtained at a field of about $\frac{1}{2}$ G. The Zeeman transitions in an optically pumped rubidium-87 sample were observed by Dehmelt's method.[1–4] The intensity of circularly polarized rubidium $D-1$ radiation (7947 Å) transmitted along the earth's magnetic field H_e through the sample was observed as a function of the frequency of a weak rf field applied perpendicular to H_e. All components of the Zeeman transitions were well resolved despite splittings of only 46 cps between transitions within the same hyperfine level. The measurements were made at the Fredericksburg Magnetic Observatory of the U. S. Coast and Geodetic Survey in order to obtain good magnetic field stability and homogeneity. A proton free-precession magnetometer which was available at the Observatory[5] was used to measure the proton resonance frequency.

The dc rubidium magnetometer[6] was designed to be as nonmagnetic and as free from systematic errors as possible. Direct interchanges of the proton resonance head and the rubidium sample were made. The main limitation on the experimental accuracy came from possible weak paramagnetism of the proton resonance coil. It was unfortunately not possible to remove the water sample from the proton magnetometer and observe the rubidium frequency inside the proton resonance coil. A self-oscillating rubidium magnetometer[7,8]

* Present address: Joint Institute for Laboratory Astrophysics, National Bureau of Standards and University of Colorado, Boulder, Colorado.

[1] H. G. Dehmelt, Phys. Rev. **105**, 1487 (1957).
[2] W. E. Bell and A. L. Bloom, Phys. Rev. **107**, 1559 (1957).
[3] T. L. Skillman and P. L. Bender, J. Geophys. Research **63**, 513 (1958).
[4] P. L. Bender, Compt. rend. 9e Colloq. Ampere, Librairie Payot, Geneva (1960).
[5] L. Hurwitz and J. H. Nelson, J. Geophys. Research **65**, 1759 (1960).
[6] The phrase "dc rubidium magnetometer" is used for convenience to denote a magnetometer in which the observed changes in optical absorption coefficient for the sample are slow compared with the Larmor precession frequency.
[7] H. G. Dehmelt, Phys. Rev. **105**, 1924 (1957).
[8] A. L. Bloom, Appl. Optics **1**, 61 (1962).